ICARUS **124,** 490–499 (1996)
ARTICLE NO. 0225

The Lunar Opposition Surge: Observations by Clementine

BONNIE J. BURATTI, JOHN K. HILLIER, AND MICHAEL WANG

Jet Propulsion Laboratory, California Institute of Technology, 4800 Oak Grove Drive, MS 183-501, Pasadena, California 91109
E-mail: buratti@jplpds.jpl.nasa.gov

Received December 4, 1995; revised May 10, 1996

The Clementine mission to the Moon in 1994 provided the first multispectral observations of the lunar opposition surge below a few degrees. The brightness of the Moon increases more than 40% between solar phase angles of 4° and 0°. The opposition effect exhibits a small wavelength dependence: the surge is ~3–4% larger at 0.41 μm than at 1.00 μm. This result suggests that the principal cause of the lunar opposition surge is shadow hiding, while coherent backscatter, if present, makes only a minor contribution. The amplitude of the effect depends significantly on terrain: the surge is about 10% greater in the lunar highlands. This difference is attributed to textural variations between the two terrains. The Clementine measurements provide a new basis for deriving spectral geometric albedos, phase integrals, and Bond albedos. A value of 0.11 ± 0.01 was found for the lunar bolometric Bond albedo. This value is at the low end of the historical published values, but not as low as the recent result of 0.080 ± 0.002.

I. INTRODUCTION

The Moon exhibits a nonlinear surge in brightness as its face becomes fully illuminated to an observer. The canonical explanation for this ''opposition surge'' is a shadow-hiding mechanism, in which mutual shadows cast by particles in the upper regolith are hidden at opposition but become rapidly visible as the phase angle increases (Irvine 1966, Hapke 1986). Because the character of the opposition effect is a sensitive indication of the surficial compaction state and particle size (Hapke 1986)—and thus of lunar geophysical processes—observations at small solar phase angles are important to obtain. Recent observations have shown that many Solar System bodies exhibit, in addition to an opposition effect that is typically seen at solar phase angles less than ~6°, extremely narrow and large surges in brightness below 1° (Buratti *et al.* 1992, Thompson and Lockwood 1992). Standard shadow-hiding models require extremely (and probably unreasonably) porous surfaces to explain these narrow opposition surges (see Domingue *et al.* 1991). Problems of this sort have led to the suggestion that a second mechanism, coherent backscatter, may be responsible for the observed surge (Hapke 1990, Mishchenko 1992). In this mechanism, photons following identical but reversed paths in a surface interfere constructively in exactly the backscattering direction leading to up to a factor of 2 increase in brightness. A narrowly peaked opposition surge was observed on lunar samples measured in the laboratory, although these measurements did not extend to phase angles less than 1° (Hapke et al. 1993).

The Moon's finite angular size as seen from Earth precludes ground-based observations of its solar phase curve below ~0.5°: at this point a lunar eclipse occurs. Previous Apollo photographic observations of the Moon suggested that the Moon has a huge opposition spike below 0.75° (Pohn *et al.* 1969, Wildey 1978). The Clementine mission enabled the first electronic, multispectral observations of the Moon at very small solar phase angles. Several hundred images of the opposition surge of the Moon under 1° were obtained by the spacecraft. This set of data is by far the most extensive for any celestial object at small solar phase angles, and they offer an unprecedented opportunity to study the opposition effect on a planetary surface. The data are of course disk resolved, and extend over the wavelength range 0.41 to 1.0 μm for the UV/Vis camera and 1.0 to 2.8 μm for the near-IR camera. Another important feature of the Clementine observations is that a change of several degrees in solar phase angle appears on one image; it is thus possible to create a highly accurate phase curve in those last few degrees. The typical scatter that appears in published phase curves at small phase angles is about 0.5 astronomical magnitude (about a factor of 2; see Helfenstein *et al.* 1996); the Clementine data exhibit scatter of ~1–5% (the variations are due primarily to albedo changes rather than error). The multispectral observations offer a critical test of the mechanism responsible for the lunar opposition surge: the shadowing mechanism should be more pronounced at wavelengths for which the albedo is lower (since shadows are not partly illuminated), whereas coherent backscatter should show the opposite relationship, because it is a multiple scattering phenomenon.

For a description of the Clementine spacecraft and its instruments, and an overview of the scientific results, see Nozette *et al.* (1994).

0019-1035/96 $18.00

TABLE I
Summary of Clementine UV/Vis Images at Opposition Used in This Study (Filters A–E)

Orbit	Image ID	Number of images
150	LUE3739J-LUA3755J	10
151	LUE3559J-LUA3575J	10
153	LUE3568J-LUA3584J	10
154	LUE3750J-LUA3766J	10
155	LUE3588J-LUA3604J	10
165	LUE1648J-LUA1694J	10
166	LUE1969I-LUA1984J	5
167	LUE2268J-LUA2283J	5
168	LUE1967J-LUA1983J	10
169	LUE2263J-LUA2279J	10

II. OBSERVATIONS AND DATA ANALYSIS

The Clementine images at small solar phase angles were obtained near the middle of the mission and near the lunar equator. We have chosen to analyze the data from the UV/Vis camera for the following reasons: the calibration factors are better understood than those for the NIR, HiRes, or LWIR cameras; it is easier to compare our results with ground-based observations of the Moon and other bodies; and the complicating factor of thermal emission is minimized. The UV/Vis is also best suited for studying the effect of albedo on the opposition surge, because the albedo of the Moon changes most significantly between ~0.4 and 0.8 μm. Table I summarizes the images used in our study. Each image was bias-subtracted and corrected for imperfections and spatial variations in charge-coupled device (CCD) sensitivity with inflight flatfields created by the Clementine science team (M. Robinson, personal communication, 1995).

In each of the images obtained at small solar phase angles, a small (~0.50° wide) bright spot appears at the point of 0°. This spot is not instrumental, and it is also seen on NIR images (a search of HiRes images has not yet been made). Figure 1 shows typical images (orbits 149 and 167); Fig. 2 presents a scan extracted from 0° to the edge of one of the images. For comparison, we show solar phase curves for other bodies that exhibit opposition surges at small solar phase angles. The surge seen by Clementine is qualitatively similar to that reported by Pohn *et al.* (1969) and Wildey (1978) on Apollo photographs, although our measurements show that the effect is somewhat greater than that derived from the photographs [43 ± 2% in the visual region of the spectrum between 4° and 0°, as opposed to 37% reported by Pohn *et al.* (1969)].

Two important factors to investigate for the lunar opposition surge are the dependence of the effect on wavelength and terrain type. Wavelength dependence is a clear indication of the mechanism responsible for the effect, whereas terrain dependence indicates differences in surface textural properties between the lunar highlands and maria. Scans of the opposition surge in the five primary filters of the UV/Vis were extracted from images in orbits 150, 151, 154, 155, 165, 166, 167, 168, and 169. The data from these images were extracted with the following procedure. First, the scattering angles (incidence, emission, and solar phase angles) at the center of each 2 × 2 block of pixels were calculated with procedures provided by the JPL Navigation Section's SPICE library. The reflectance from each group of 4 pixels was then averaged (the averaging procedure was required to save disk space). The data for each image were then binned in 0.02° increments of phase angle, and the resulting averaged data were normalized such that the average reflectance in the lowest bin (0–0.02°) is 1.0. The data for all images for each filter were then added together. The resulting averaged lunar opposition surges at 0.41, 0.75, and 1.0 μm, representing the full range in wavelength for the UV/Vis camera, are shown in Fig. 3a. To quantify the dependence of the surge on wavelength, a line was fit to the composite phase curves between 0° and 4° (brightness = $A + B\alpha$; see Table II). The values show that the amplitude of the surge is inversely correlated with wavelength, although by a small amount. At a phase angle of 4°, this effect is most clearly seen: the reflectance is 0.690 for filter A (0.41 μm), 0.703 for filter B (0.75 μm), 0.715 for filter C (0.90 μm), 0.720 for filter D (0.95 μm), and 0.715 for filter E (1.00 μm) (Table III). This effect of "phase reddening" has been described previously for the Moon and other bodies (e.g., Lane and Irvine 1973) at larger phase angles. Because of the increase in the Moon's albedo with wavelength from visible to near-IR wavelengths, the shadow-hiding mechanism predicts that the opposition surge is inversely correlated with wavelength to produce a reddening of the lunar albedo as the phase angle increases (Irvine 1966, Helfenstein *et al.* 1996). With increasing albedo, multiply scattered photons cause partial illumination of shadows. Early measurements (Mikhail 1970) confirm the prediction. The observations by Gehrels *et al.* (1964) over 11 lunar regions at the very smallest

TABLE II
Fits of Curves to $A + B\alpha$

Filter	λ_{eff} (μm)	Bandpass (FWHM) (μm)	A (±0.01)	B (±0.002)
A	0.41	0.036	1.00	−0.078
B	0.75	0.0093	1.00	−0.076
C	0.90	0.0185	1.00	−0.075
D	0.95	0.0287	1.00	−0.075
E	1.00	0.0282	0.99	−0.072

TABLE III
Wavelength-Dependent Geometric Albedos (p_λ), Bond Albedos ($A_{B\lambda}$), and Phase Integrals (q_λ), with Some Previous Values for Comparison

Filter	0°/4° (±0.01)	p_λ[a] (±0.005)	p_λ[b]	p_λ[c]	q_λ[a] (±0.005)	q_λ[b]	q_λ[c]	$A_{B\lambda}$[a] (±0.01)	$A_{B\lambda}$[b]	$A_{B\lambda}$[c]
A	1.45	0.116	0.088	0.09	0.45	0.551	0.46	0.052	0.048	0.041
B	1.42	0.233	0.179	0.15	0.50	0.633	0.54	0.117	0.113	0.081
C	1.40	0.232	0.195	0.14	0.53		0.65	0.123		0.091
D	1.39	0.230	0.195	0.13	0.54		0.67	0.124		0.087
E	1.40	0.260	0.202	0.13	0.55	0.676	0.70	0.143	0.136	0.091

[a] This study; q_λ for filters C and D interpolated.
[b] Lane and Irvine (1973); correspondences made as follows: $A \equiv 4155$ Å, $B \equiv 7297$ Å, $E \equiv 10635$ Å; corresponding values for p_λ in filters C and D interpolated from their Fig. 7.
[c] Helfenstein *et al.* (1996); p_λ and q_λ from their Fig. 7.

phase angles (2°–0.8°) show no clear trend. Goniometric measurements on an Apollo 11 sample from Tranquility Base show an inverse phase reddening (O'Leary and Briggs 1970) under 5°. In the most comprehensive prior study of the wavelength dependence of the opposition surge, Helfenstein *et al.* (1996) conclude that the strength of the surge decreases with increasing albedo; however, their color data include no observations below 5°. Our measurements are the first to suggest phase reddening of the opposition surge for the Moon as a whole for small phase angles ($< 5°$). The measured effect is small, but within our errors. At the Moon's low albedo, multiple scattering is not significant and phase reddening should be small (see Sections III and IV). To further illustrate the small dependence of the opposition curve on wavelength, we show typical color ratios of individual regions, with their linear best-fit curves (Fig. 3b). Within the errors, the slope of the lines is zero. The effect is so small that many curves must be coadded to bring it above the confounding effects of topography and albedo.

A correlation between lunar terrain type and the character of the opposition surge was reported by Wildey and Pohn (1969), who show that the surge near Tranquility Base is only 7% between phase angles of 1.5° and 0°, whereas the surge for the Moon as a whole from Apollo photogrammetry is 19% over the same range. Gehrels *et al.* (1964) measured opposition surges on 13 separate regions (the minimum phase angle ranged from 0.8° to 1.0°). Although the amplitude and width of the effect vary from region to region, no clear trend with terrain type, albedo, etc., is evident. To derive a possible correlation between the lunar opposition surge and the two major terrain types (highlands and maria), we constructed composite curves representing these areas. Images obtained at 0° phase angle in orbit 167 are located in the highland regions near 5°E. longitude, while orbit 152 contains images of the opposition surge in Mare Tranquilitatis (both regions are near the equator, where all the opposition images are located). Figure 4 shows the two composite curves and a ratio of the highland to maria regions (because most images have a mixture of the two terrain types, we were able to construct well-averaged curves for $\alpha \leq 1.2°$ only). Clearly, there is a trend, with the amplitude of the surge about 10% greater for the highlands. This trend is in the same direction as that reported by Wildey and Pohn (1969), although our measurements do not show as significant an effect; our data reveal a surge of 16% between 1.2° and 0° for Mare Tranquilitatis, compared with Wildey and Pohn's (1969) measurement of only 7% between 0° and 1.5°.

The Clementine spacecraft's observations of the lunar opposition effect enable an accurate measurement of the Moon's geometric albedo (p), phase integral (q), and Bond albedo (A_B). By definition, the geometric albedo can be known only from observations at opposition. In their extensive study of the integral geometric albedo of the Moon, Lane and Irvine (1973) point out that the values they derived based on a linear extrapolation of the lunar phase curve were underestimated by a factor of 44 to 100%. Similarly, Helfenstein *et al.* (1996) obtain an estimate of the normal reflectance (which is very nearly equal to the geometric albedo in the case of the Moon) that is 50% uncertain (their Fig. 1c). Their values for p and q (Helfenstein *et al.,* 1996, Fig. 7) are based on a fit to a Hapke-type model.

A composite lunar phase curve for three colors is illustrated in Fig. 5; the data between 0° and 4° are from the Clementine UV/Vis camera, whereas the remaining data are from Lane and Irvine (1973); the data for each color are normalized at 4°. Table III lists the corresponding geometric albedos in the Clementine filters; these geometric albedos are based on those obtained by Lane and Irvine (1973), but with Clementine's measured opposition surge. Future work, making use of the full calibration of the Clementine cameras, will yield a direct measurement of

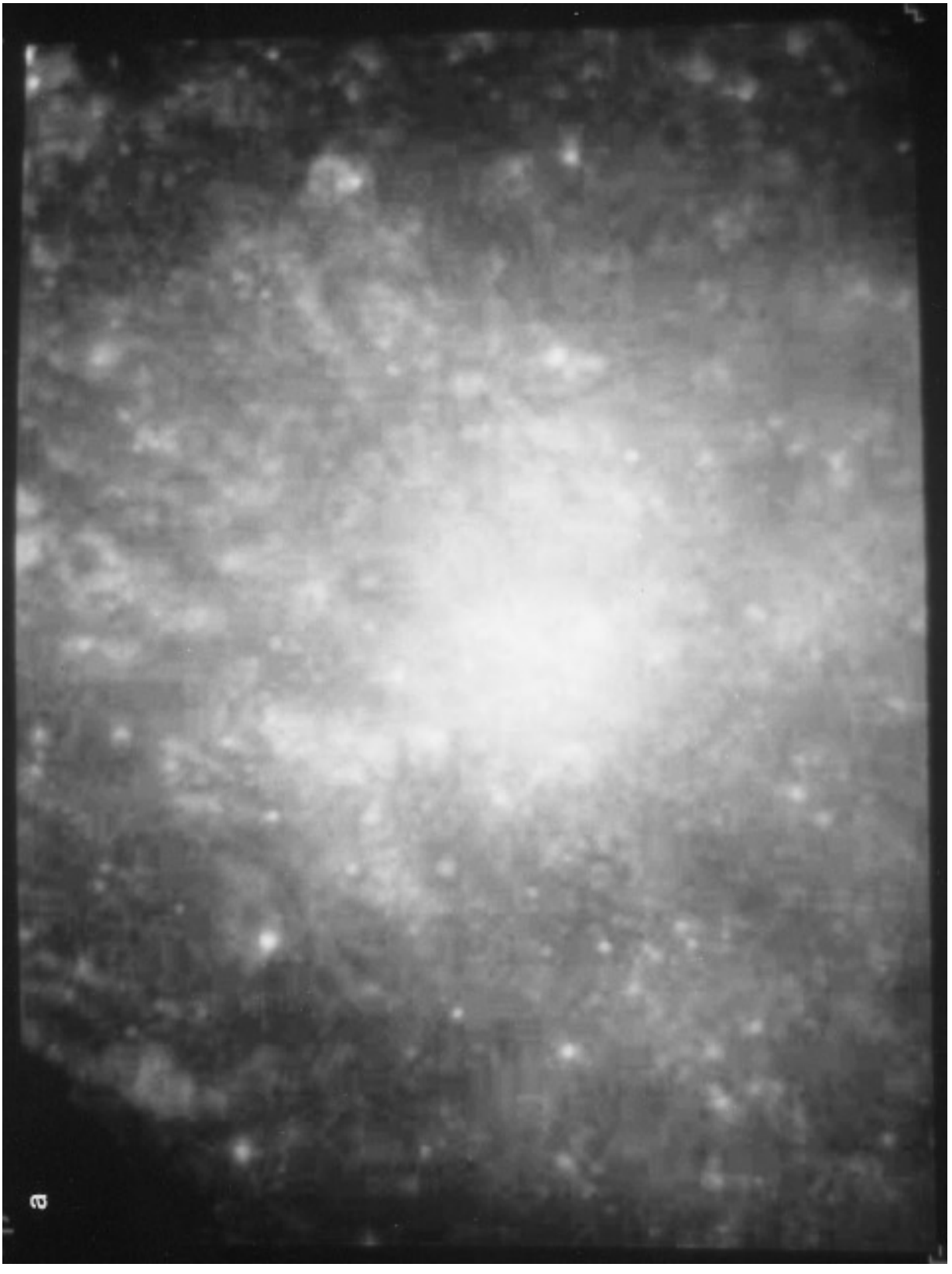

FIG. 1. Images illustrating typical examples of opposition surges seen by the Clementine spacecraft: (a) Image LUC11225, in orbit 167, near 1°N latitude and 4°E longitude, in the lunar highlands at the east edge of Sinus Medii. (b) Images LUC30017 (top) and LUC30079 (bottom) in orbit 149, located in Mare Fecunditatis near latitudes and longitudes of 0°, 50°E and 1°N, 51.5°E, respectively. In image LUC30017 the surge is the bright spot in the middle left side of the image (above the bright impact crater); in image LUC 30079 it is in the upper middle left area of the picture. (The blocky artifacts are due to lossy data compression.)

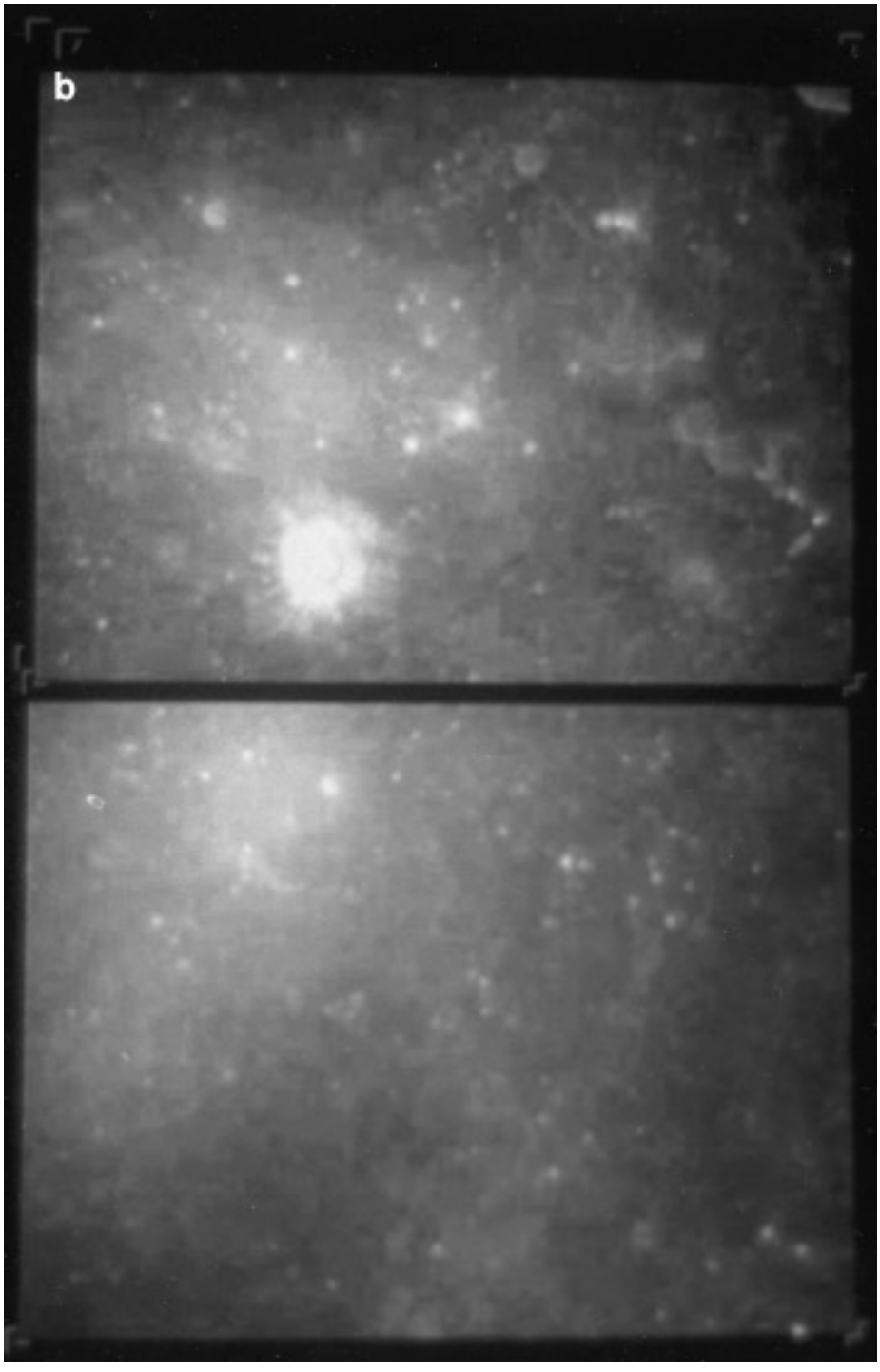

FIG. 1—*Continued*

the geometric albedo. Although there were no Clementine filters corresponding to the astronomical visual filter (0.55 μm), the interpolated value for the visual geometric albedo is 0.16 ± 0.01. This value is higher than those of 0.14–0.15 obtained previously (Helfenstein and Veverka 1987, Lumme and Irvine 1982).

The phase integral (Russell 1916) was computed with a 2-point Gaussian quadrature (Chandrasekhar 1960) for the three phase curves in Fig. 5. The resulting values, along with the Bond albedo ($A_B = p * q$), are listed in Table IV with previous values for comparison. At the visual wavelengths, the increase in geometric albedo is offset by a

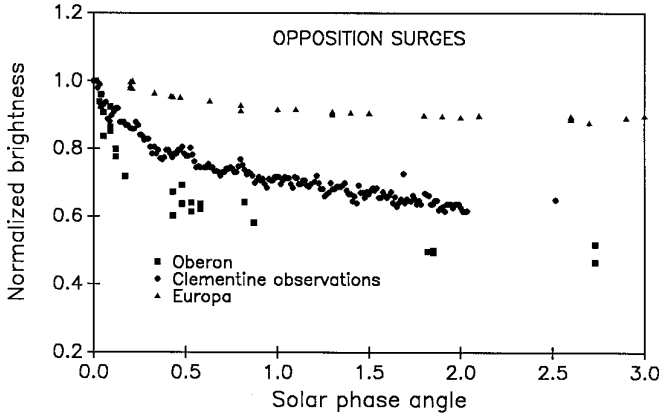

FIG. 2. Scan of the opposition surge extracted from the image in Fig. 1a. For comparison, the opposition phase curves of Oberon (Buratti *et al.* 1992) and Europa (Thompson and Lockwood 1992).

decrease in the phase integral, so that the new values of the Bond albedo are not very different from those of Lane and Irvine (1973), although our values are higher than those of Helfenstein *et al.* (1996). In the near-IR (1.0 μm) our value for the lunar Bond albedo is significantly higher than previous estimates.

The bolometric (or radiometric) Bond albedo, an important quantity for understanding the thermal properties of the Moon, is given by

$$A_B = \int_0^\infty F_\odot(\lambda) p_\lambda q_\lambda \, d\lambda \Big/ \int_0^\infty F_\odot(\lambda) \, d\lambda, \qquad (1)$$

where $F_\odot(\lambda)$ is the flux of the Sun at wavelength λ. The values of q were interpolated for filters C and D (see Table III). For p and q between 1.0 and 2.5 μm, we extrapolated from our values with a wavelength dependency derived from Helfenstein *et al.* (1996). Using the values for the flux of the Sun listed in Allen (1976), we find a bolometric Bond albedo of 0.11 $\pm$ 0.01, based on data between 0.41 and 2.5 μm. This value is at the low range of previously published values of 0.11–0.136 (Lane and Irvine 1973 and references cited therein, Helfenstein and Veverka 1987), but not as low as the value of 0.080 $\pm$ 0.002 recently derived by Helfenstein *et al.* (1996). Our value is lower than most previous values because we have fully included the opposition surge, but it is still higher than the value of Helfenstein et al. because of our different spectral dependencies for p and q (see Table III) in the visible. Helfenstein and coworkers' values for p ultimately depend on laboratory measurements of Apollo samples, which might have been redder than the Moon as a whole, with corresponding lower Bond albedos. Some of the discrepancy may be due to systematic offsets between model-derived parameters (Helfenstein *et al.* 1996) and measured parameters (this study).

III. MODELING

The color-dependent opposition curves provided by Clementine render the first opportunity to critically test which mechanism is responsible for the opposition surge. According to the shadow-hiding model, the width of the opposition surge depends primarily on the porosity of the surface and, therefore, should be relatively independent of wavelength (in the case of bodies for which multiple scattering is important, and which have increasing albedos with wavelength, the surge should become less significant with increasing wavelength). Figure 6 illustrates the quantitative prediction of the wavelength dependence of the shadow-hiding model. Over the range of single scattering albedos for the Moon between 0.4 and 1.0 μm (0.2–0.4, Helfenstein *et al.* 1996), the expected effect is about 1%. Although small, the effect is in good agreement with actual measurements (Table II; and Table III, column 2) In contrast, the coherent backscatter model predicts a strong wavelength dependence to the opposition surge. These differences provide a diagnostic we can use to help distinguish which mechanism is most responsible for the observed surge. Our result that there is only a small color dependence to the lunar opposition surge (Fig. 3a and Table II) suggests that coherent backscatter is not the dominant mechanism for the Moon's surge in brightness. Moreover, the dependence is in the wrong direction. Mishchenko (1992) suggests that the wavelength dependence of coherent backscatter might disappear if there is a wide distribution of particle sizes, but only for icy surfaces. For silicate surfaces, the effect remains "substantially wavelength-dependent."

A shadow-hiding model can provide a reasonable fit to the lunar opposition phase curve. Table IV lists our best-fit values to the Clementine data for Hapke's (1986) compaction parameter, h, in each filter. [The porosity, P, of the optically active portion of the surface is related to h by $h = -3/8(\ln(P)) \cdot Y(r)$, where $Y(r)$ is a function of the particle size distribution $h(r)$ (Hapke 1986).] Figure 7 shows that an h of $\sim$0.04 can provide a good fit to the lunar opposition surge in reasonable agreement with previously determined values of h = 0.05–0.07 found from data at larger phase angles (Hapke 1986, Helfenstein and Veverka 1987, Helfenstein *et al.* 1996). For reasonable particle size distributions, such values can yield reasonable surface porosities (Hapke, 1986). This suggests that shadow hiding alone can adequately describe the lunar opposition surge at all phase angles. In addition to Hapke's model, we have recently developed a modified shadow-hiding model based on his model, except it allows for two-layer surfaces in which the particle properties (e.g., particle size) can vary between the layers (Hillier 1996). Figure 7 shows that the modified model can also provide a good fit to the lunar opposition surge data while requiring less porous surfaces

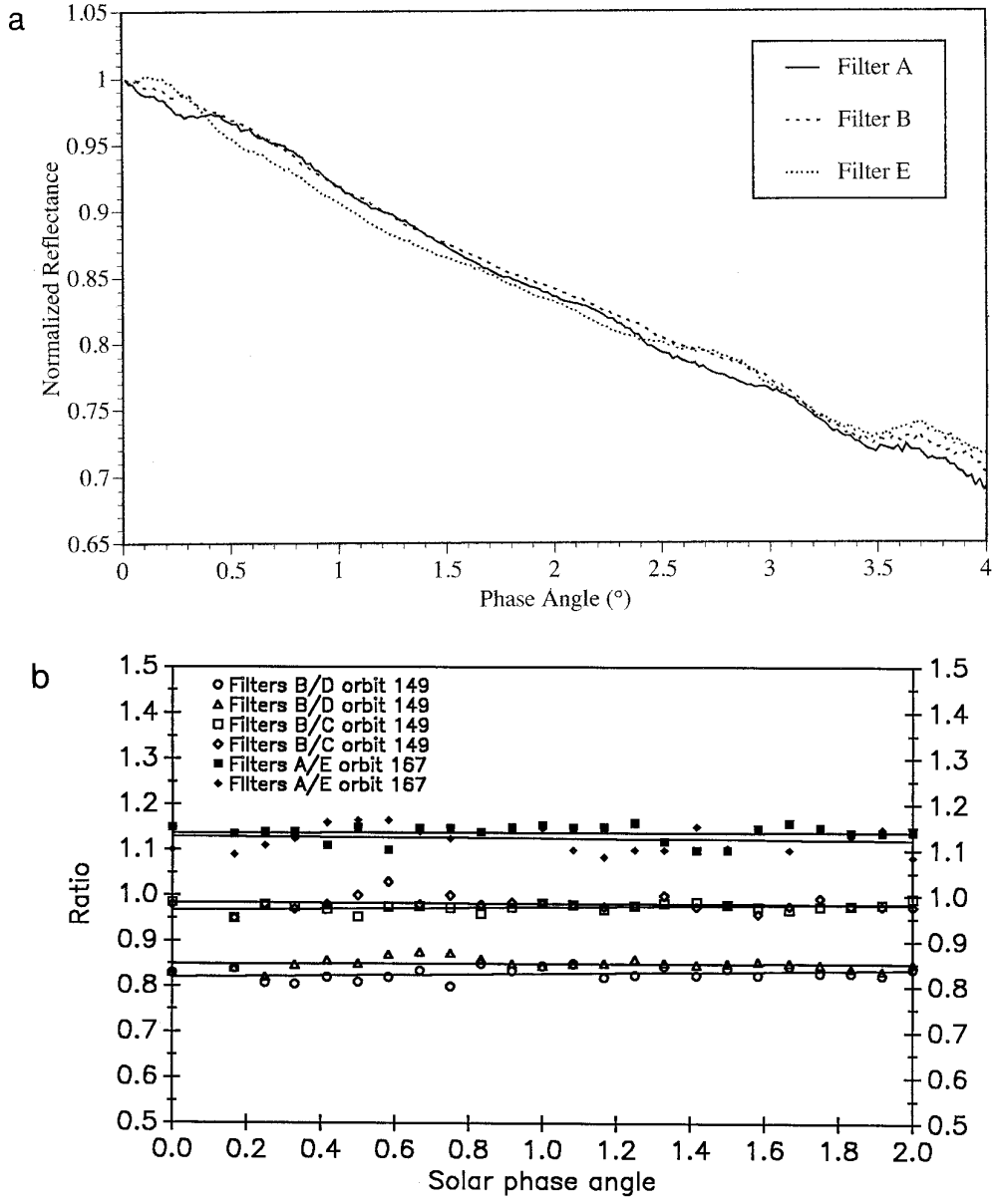

FIG. 3. (a) Averaged opposition phase curves of the Moon in three Clementine filters representing the wavelength range of the UV/Vis camera (for clarity the other two filters are not included). Some structure still exists due to albedo variegations and topography. (b) Color ratios between various filters for individual regions. Each line is an ratio of scans in two filters. The open symbols represent orbit 149, in Mare Fecunditatis; the filled symbols, orbit 167, in the highlands east of Sinus Medii. The lines are linear best fits for each ratio. To offset the effects of topography, 8-point running averages are shown. For clarity, filters A/E are offset by 0.1.

than the standard shadow hiding model if the particle size decreases toward the surface. Apollo core samples show the lunar surface to be relatively well mixed, with grain size relatively independent of depth (though with a slight suggestion of decreasing particle size toward the surface; McKay *et al.* 1977, 1991); however, the upper millimeter or so (a significant fraction of the optically active surface) of the regolith is expected to undergo intense micrometeoritic bombardment (Gault *et al.* 1974). While it is not entirely clear whether such bombardment would lead to smaller particles, soil maturation models do suggest a decrease in particle size with maturity (McKay *et al.* 1991). Even if it is not necessary to explain the lunar opposition surge, the two-layer model may provide an alternative to coherent backscatter as an explanation for the extremely narrow opposition surges observed on several other Solar System bodies (Fig. 2).

Another possibility, which may exist in conjunction with shadow hiding, is that properties of individual particles cause them to have sharply peaked single-particle-phase

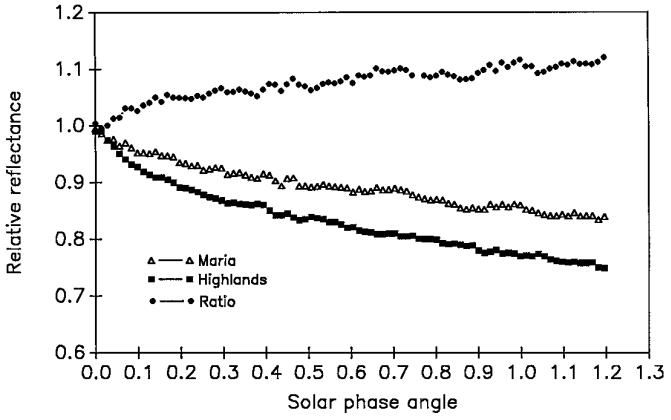

FIG. 4. Averaged opposition phase curves of the lunar maria (triangles) and highlands (filled squares). The ratio of maria/highlands (filled circles) shows that the highlands exhibit a surge about 10% higher than that of the maria in the last degree.

functions. Since these two effects are due to singly scattered photons only, they are indistinguishable.

IV. CONCLUSIONS AND DISCUSSION

The Clementine spacecraft provided the first multispectral observations of the lunar opposition effect. Between 4° and 0° the brightness of the Moon increases by about 40–45%. The amplitude of the surge depends weakly on wavelength; the blue region of the spectrum exhibits a ~3–4% larger effect. There is a significant dependence of the opposition surge on lunar terrain type. On average, the opposition surge in the lunar maria is about 10% less than that seen in the highlands. If this difference is attributed to textural properties, it means the highlands are more tenuous than the maria. The textural difference could be attributed to the longer period of micrometeoritic bombardment to which the highlands have been subjected. McKay *et al.* (1974) present a model in which the highlands have finer particles because the excavation of large boulders from a deeper bedrock is less likely.

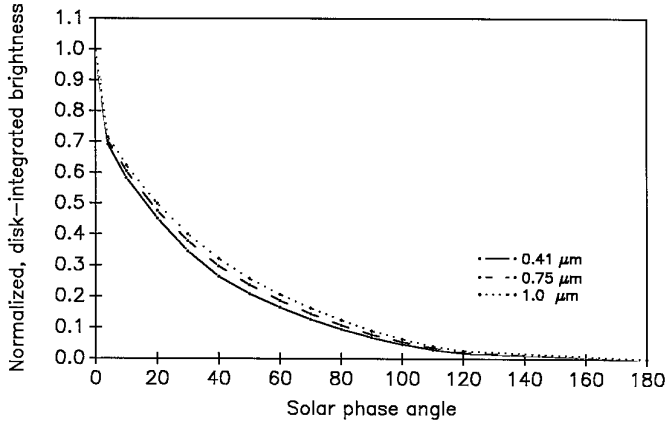

FIG. 5. Integral phase curve of the Moon at three wavelengths. The small phase angles (<5°) were derived from Clementine data, whereas the larger phase angles were adopted and renormalized from Lane and Irvine (1973).

TABLE IV
Best Fit Compaction Parameters for Each of the Clementine Filters

Filter	h (±0.04)
A	0.039
B	0.041
C	0.044
D	0.043
E	0.042

If coherent backscatter is important on the Moon, the opposition surge would be more pronounced in the Clementine E filter (1.0 μm), where the degree of multiple scattering should be the highest. This is definitely not the case. We conclude on the basis of this observation that shadow hiding is the primary mechanism for the surge. Canonical shadow-hiding models (Hapke 1986, which draws on the earlier work of Irvine 1966 and Seeliger 1887), as well as a new two-layer model of shadow hiding (Hillier 1996), yield reasonable values for the lunar porosity (~70%). The fact that there is only a small spectral dependence to the opposition surge means that multiple scattering is not important on the Moon. If it were, and shadow hiding were the principal mechanism, the red wavelengths should exhibit significantly smaller surges, because the shadows would be partly illuminated by multiply scattered photons. At every wavelength, only primary shadows are created.

Laboratory experiments on the photometric effects of multiple scattering do indeed show that a photometric model involving only singly scattered radiation applies to surfaces with normal reflectances less than 0.30 (Veverka *et al.* 1978). For the Saturnian satellites, multiple scattering is not important unless the normal reflectance is greater than ~0.60 (Buratti 1984). The fact that multiple scattering is unimportant on the Moon has been known for more than 100 years: the solution to the equation of radiative transfer for single scattering from a surface is the well-known Lommel–Seeliger photometric function of the Moon. Similarly, near opposition the Moon is known to exhibit no limb darkening, the signature of multiple scattering (Schoenberg 1925, Minnaert 1961). It is thus not surprising that coherent backscatter, a phenomenon that depends on multiple scattering, is not the principal mechanism for the lunar opposition surge.

Although our results suggest that shadow hiding (or

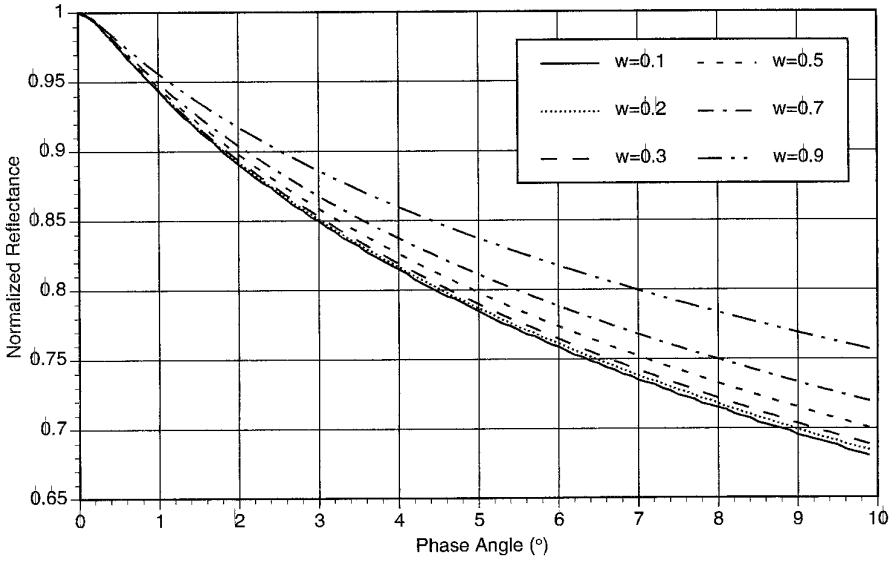

FIG. 6. Predicted opposition curves of the shadow-hiding model as a function of single scattering albedo (w). The effect of albedo on the phase curves is significant for $w > 0.5$. The Henyey–Greenstein $g = -0.3$.

possibly an intrinsically peaked single-scattering phase function) is primarily responsible for the opposition surge seen on the Moon, it would be premature to say the effect of coherent backscatter is entirely absent. Laboratory measurements of Apollo samples down to 1° show the polarization signature expected for coherent backscatter (Hapke *et al.* 1993). Similarly, there is still the possibility that the terrain difference exhibited is due to higher reflectances in the lunar highlands, rather than textural properties.

The Clementine measurements of the opposition effect provide the first accurate multispectral phase curve of the Moon at small phase angles. When combined with ground-based observations at higher phase angles, more accurate values of fundamental photometric and radiometric properties can be derived. The surge means that the spectral geometric albedo of the Moon is higher than previously realized, whereas the wavelength-dependent phase integral is lower. Our bolometric Bond albedo of 0.11 ± 0.01

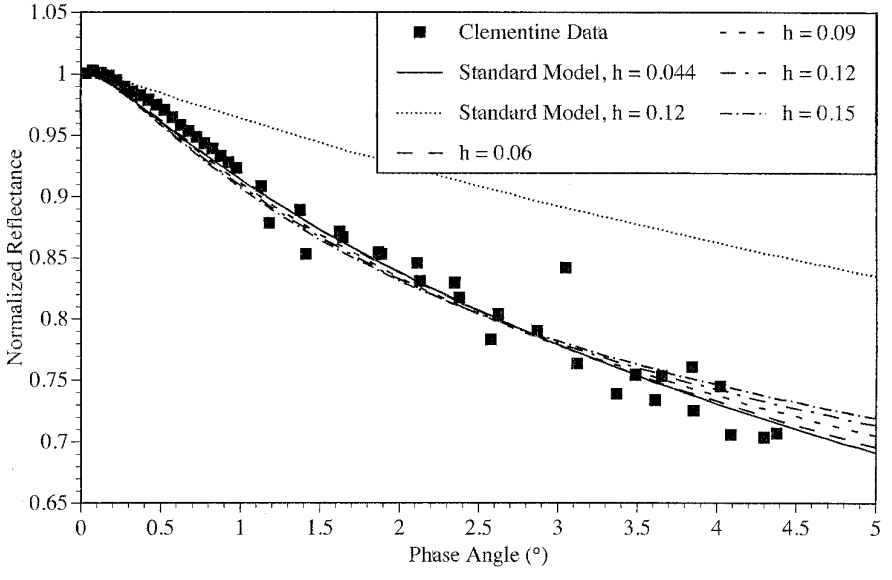

FIG. 7. Fit of standard (dotted and solid lines) and two-layer shadow-hiding (remaining four lines) models to Clementine data at small solar phase angles. Shown are fits for various values of Hapke's (1986) opposition surge width parameter, h. In these models, the single-scattering albedo $w = 0.245$ for both layers, and the ratio of particle sizes in the two layers is (corresponding from lowest to highest value of h): 0.63, 0.29, 0.19, and 0.14. We have accounted for the finite size of the Sun as seen from the Moon in the model.

is at the low range of previous values, but not as low as the value of 0.080 ± 0.002 found by Helfenstein *et al.* (1996).

ACKNOWLEDGMENTS

We thank Bruce Hapke and Alfred McEwen for their detailed reviews of our paper. This work was performed at the Jet Propulsion Laboratory, California Institute of Technology, under contract with the National Aeronautics and Space Administration. This work was performed while J. K. Hillier held a National Research Council Resident Research Associateship at the Jet Propulsion Laboratory.

REFERENCES

Allen, C. W. 1976. *Astrophysical Quantities.* Athlone Press, London.

Buratti, B. J. 1984. Voyager disk resolved photometry of the saturnian satellites. *Icarus* **59,** 392–405.

Buratti, B. J. 1985. Application of a radiative transfer model to bright icy satellites. *Icarus* **61,** 208–217.

Buratti, B. J., J. Gibson, and J. Mosher 1992. CCD observations of the uranian satellites. *Astron. J.* **104,** 1618–1622.

Buratti, B. J., W. Smythe, R. M. Nelson, and V. Gharakhani 1988. Spectrogoniometer for measuring planetary surface materials at small phase angles. *Appl. Opt.* **27,** 161–165.

Chandrasekhar, S. 1960. *Radiative Transfer*. Dover, New York.

Domingue, D. L., B. W. Hapke, G. W. Lockwood, and D. T. Thompson 1991. Europa's phase curve: Implications for surface structure. *Icarus* **90,** 30–42.

Gault, D. E., F. Horz, D. E. Brownlee, and J. B. Hartung 1974. Mixing of the lunar regolith. *Proc. Lunar Sci. Conf. 5th,* 2365–2386.

Gehrels, T., T. Coffeen, and D. Owings 1964. Wavelength dependence of polarization: III. The lunar surface. *Astron. J.* **69,** 826–852.

Goguen, J. D. 1996. A quantitative test of the applicability of independent scattering to high albedo planetary regoliths. *Icarus*, submitted.

Hapke, B. 1966. An improved lunar theoretical photometric function. *Astron. J.* **71,** 333–339.

Hapke, B. 1986. Bidirectional reflectance spectroscopy. 4. The extinction coefficient and the opposition effect. *Icarus* **67,** 264–280.

Hapke, B. 1990. Coherent backscatter and the radar characteristics of outer planet satellites. *Icarus* **88,** 407–417.

Hapke, B., R. M. Nelson, and W. Smythe 1993. The opposition effect of the Moon: The contribution of coherent backscatter. *Science* **260,** 509–511.

Helfenstein, P., and J. Veverka 1987. Photometric properties of lunar terrains derived from Hapke's equation. *Icarus* **72,** 342–357.

Helfenstein, P., J. Veverka, J. Hillier, C. M. Pieters, S. Pratt, J. W. Head, G. Neukum, H. Hoffmann, and A. Oehler 1996. The wavelength dependence of lunar photometric properties. *Icarus*, submitted.

Hillier, J. 1996. Shadow hiding opposition surge for a two-layer surface. *Icarus,* submitted.

Hillier, J., P. Helfenstein, A. Verbiscer, J. Veverka, R. H. Brown, J. Goguen, and T. V. Johnson 1990. Voyager disk-integrated photometry of Triton. *Science* **250,** 419–421.

Irvine, W. M. 1966. The shadowing effect in diffuse radiation. *J. Geophys. Res.* **71,** 2931–2937.

Lane, A., and W. Irvine 1973. Monochromatic phase curves and albedos for the lunar disk. *Astron. J.* **78,** 267–277.

Lumme, K., and W. Irvine 1982. Radiative transfer in the surfaces of atmosphereless bodies: III. Interpretation of lunar photometry. *Astron. J.* **87,** 1076–1082.

McKay, D. S., M. A. Dungan, R. V. Morris, and R. M. Fruland 1977. Grain size, petrology, and FMR studies of the double core 60009/10: A study of soil evolution. *Proc. Lunar Sci. Conf. 8th,* 2929–2952.

McKay, D. S., R. M. Fruland, and G. H. Heiken 1974. Grain size and the evolution of lunar soils. *Proc. Lunar Sci. Conf. 5th,* 887–906.

McKay, D. S., G. Heiken, A. Basu, G. Blanford, S. Simon, R. Reedy, B. M. French, and J. Papike 1991. The lunar regolith. In *The Lunar Sourcebook* (G. H. Heiken, D. T. Vaniman, and B. M. French, Eds.), pp. 285–356. Cambridge Univ. Press, New York.

Mikhail, J. S. 1970. Colour variations with phase of selected regions of the lunar surface. *Moon* **2,** 167–201.

Minnaert, M. 1961. Photometry of the Moon. In *The Solar System. III. Planets and Satellites.* (G. P. Kuiper and B. M. Middlehurst Eds.). Univ. of Chicago Press, Chicago.

Mishchenko, M. I. 1992. The angular width of the coherent backscatter opposition effect: An application to icy outer planet satellites. *Astrophys. Space Sci.* **194,** 327–333.

Nozette, S., and 33 colleagues 1994. The Clementine mission to the Moon: Scientific overview. *Science* **206,** 1835–1839.

O'Leary, B., and F. Briggs 1970. Optical properties of Apollo 11 Moon samples. *J. Geophys. Res.* **75,** 6532–6538.

Pohn, H. A., H. W. Radin, and R. L. Wildey 1969. The Moon's photometric function near zero phase angle from Apollo 8 photography. *Astrophys. J.* **157,** L193-L195.

Russell, H. N. 1916. On the albedo of planets and their satellites. *Astrophys. J.* **43,** 173–195.

Schoenberg, E. 1925. Untersuchungen zur Theorie der Beleuchtung des Mondes auf Grund photometrischer Messungen. *Acta Soc. Sci. Fenn.* **9,** 6–71.

Seeliger, H. 1887. Zur Theorie Beleuchtung der grossen Planeten insbesondere des Saturn. *Abhandl. Bayer. Akad. Wiss. Math. Naturw. Kl. II* **16,** 405–516.

Thompson, D. T., and G. W. Lockwood 1992. Photoelectric photometry of Europa and Callisto, 1976–1991. *J. Geophys. Res.* **97,** 14761–14772.

Veverka, J., J. Goguen, S. Yang, and J. Elliot 1978. Scattering of light from particulate surfaces I. A laboratory assessment of multiple scattering effects. *Icarus* **34**, 406–414.

Wildey, R. L. 1978. The Moon in heiligenschein. *Science* **200,** 1265–1267.

Wildey, R. L., and H. A. Pohn 1969. The normal albedo of the Apollo 11 landing site and intrinsic dispersion in the lunar heiligenschein. *Astrophys. J.* **158,** L129-L130.